



Published in final edited form as:

*Clin Cancer Res.* 2008 June 15; 14(12): 3840–3849. doi:10.1158/1078-0432.CCR-07-4076.

## Affibody Molecules for *In vivo* Characterization of HER2-Positive Tumors by Near-Infrared Imaging

Sang Bong Lee<sup>1</sup>, Moinuddin Hassan<sup>2</sup>, Robert Fisher<sup>3</sup>, Oleg Chertov<sup>3</sup>, Victor Chernomordik<sup>2</sup>, Gabriela Kramer-Marek<sup>1</sup>, Amir Gandjbakhche<sup>2</sup>, and Jacek Capala<sup>1</sup>

<sup>1</sup>Radiation Oncology Branch, Center for Cancer Research, National Cancer Institute, National Institute of Child Health and Human Development, NIH, Bethesda, Maryland <sup>2</sup>Section on Biomedical Stochastic Physics, Laboratory of Integrative and Medical Biophysics, National Institute of Child Health and Human Development, NIH, Bethesda, Maryland <sup>3</sup>Protein Chemistry Laboratory, SAIC-Frederick, Inc., NCI-Frederick, Frederick, MD

### Abstract

**Purpose**—HER2 overexpression has been associated with a poor prognosis and resistance to therapy in breast cancer patients. We are developing molecular probes for *in vivo* quantitative imaging of HER2 receptors using near-infrared optical imaging. The goal is to provide probes that will minimally interfere with the studied system, i.e., whose binding does not interfere with the binding of the therapeutic agents, and whose effect on the target cells is minimal.

**Experimental Design**—We used three different types of HER2-specific Affibody molecules [monomer Z<sub>HER2:342</sub>, dimer (Z<sub>HER2:477</sub>)<sub>2</sub>, and albumin-binding domain-fused-(Z<sub>HER2:342</sub>)<sub>2</sub>] as targeting agents, and labeled them with Alexa Fluor dyes. Trastuzumab was also conjugated, using commercially available kits, as a standard control. The resulting conjugates were characterized *in vitro* by toxicity assays, Biacore affinity measurements, flow cytometry, and confocal microscopy. Semi-quantitative *in vivo* near-infrared optical imaging studies were carried out using mice with subcutaneous xenografts of HER2-positive tumors.

**Results**—The HER2-specific Affibody molecules were not toxic to HER2-overexpressing cells and their binding to HER2 did not interfere with either binding nor effectiveness of trastuzumab. The binding affinities and specificities of the Affibody-Alexa Fluor fluorescent conjugates to HER2 were unchanged or minimally affected by the modifications. Pharmacokinetics and biodistribution studies showed the albumin-binding domain-fused-(Z<sub>HER2:342</sub>)<sub>2</sub>-Alexa Fluor 750 conjugate to be an optimal probe for optical imaging of HER2 *in vivo*.

**Conclusion**—Our results suggest that Affibody-Alexa Fluor conjugates may be used as a specific near-infrared probe for the non-invasive semi-quantitative imaging of HER2 expression *in vivo*.

### Keywords

HER2; Affibody; Optical imaging; Near-infrared; Tumor targeting

---

Corresponding Author: Dr. Jacek Capala, 10 Center Dr. Building 10, Room 1B-37A, Bethesda, MD 20892, 301-435 5882 (phone), 301-480 5532 (fax), capalaj@mail.nih.gov.

Supplementary data for this article are available at Clinical Cancer Research Online (<http://clincancerres.aacrjournals.org/>).

## INTRODUCTION

Increased HER2 receptor expression, associated with resistance to therapy and with a poor prognosis, has been shown in 20–30% of breast cancers (1, 2). Therefore, HER2 has been an attractive target for molecular therapies (3). One of the most successful approaches is using HER2-specific antibodies, such as trastuzumab or pertuzumab, to prevent HER2 activation (4). Currently, the molecular therapies aimed at HER2 are often combined with conventional chemo- and/or radiotherapies (5). Extensive preclinical and clinical studies are required to optimize such combinations. One of the parameters assessed in these studies is the HER2 expression level following different therapeutic interventions (6). Thus, there is a need for molecular probes to monitor *in vivo* the receptor down-regulation as an immediate response to these therapies because the current *ex vivo* analyses of tumor tissues obtained by surgery or biopsy from breast cancer patients are not always representative (7, 8). Molecular imaging using these probes could provide an ideal noninvasive, quantitative, repetitive imaging technique (9). Traditional approaches using antibodies or antibody fragments have been proposed to address this problem (10, 11). However, these probes should minimally affect the studied system, not interfere with the binding of the therapeutic agents, and minimally affect the target cells (12).

Recently, several successful tumor imaging studies have been reported using radiolabeled HER2-specific Affibody molecules for imaging of HER2-expressing tumors (13). These very stable and highly water-soluble  $\alpha$ -helical proteins are relatively small (8.3 kDa) and can be readily expressed in bacterial systems or produced by peptide synthesis (14). Imaging agents based on those molecules will have a high affinity for HER2 and a smaller size compared to antibodies (20 $\times$ ) or antibody fragments (4 $\times$ ) and, therefore, should provide better results than the currently tested conjugates (15, 16). Furthermore, binding of the HER2-specific Affibody to an epitope that is not the target for trastuzumab enables monitoring of receptor expression following treatment with trastuzumab (17).

Optical imaging is the modality of choice for preclinical studies. It allows visualization of subcellular structures on a microscopic scale, even *in vivo*, and the macroscopic distribution of fluorescent labels in small animals (18, 19). However, high tissue autofluorescence and limited tissue penetration preclude the use of visible light for most *in vivo* imaging applications. Near-infrared (NIR) light solves these problems by reducing fluorescence background and enhancing tissue penetration (20). Over the past several years, there has been an explosion of reports describing successful *in vivo* NIR fluorescence imaging. Although most of these studies are qualitative, quantitative methods are beginning to emerge (21). Both antibodies and small molecules have been conjugated to NIR fluorophores to create tumor-specific NIR fluorescence contrast agents; although a longer washout time was required for an optimal signal-to-background ratio (22, 23). In this regard, HER2-specific Affibody molecules could be good candidates for NIR optical imaging due to their specific tumor targeting and fast body clearance, previously shown in several radionuclide imaging studies with HER2-positive tumor xenografts (24, 25).

In the present study, three different types of HER2-specific Affibody molecules were site-specifically conjugated at their C-terminal cysteine residues with Alexa Fluor dyes and compared to Alexa Fluor-labeled trastuzumab in terms of affinity and specificity to the HER2 receptor *in vitro* and *in vivo*. We also compared them using a quantitative NIR fluorescence imaging system to assess the *in vivo* application of these probes in HER2-positive tumor xenografts. Here, we report for the first time that the albumin-binding domain-fused bivalent HER2-specific Affibody can be used for *in vivo* NIR optical imaging.

## MATERIALS AND METHODS

### Reagents

The HER2-specific Affibody proteins, Affibody® monomer  $Z_{\text{HER2:342}}$  and C-terminal cysteine added forms of Affibody® His<sub>6</sub>- $Z_{\text{HER2:342}}$ -Cys (*Mr.* 8318), dimer His<sub>6</sub>-( $Z_{\text{HER2:477}}$ )<sub>2</sub>-Cys (*Mr.* 14862) and albumin binding domain added ABD-( $Z_{\text{HER2:342}}$ )<sub>2</sub>-Cys (*Mr.* 19213) were kindly provided by Affibody AB (Bromma, Sweden). All other reagents were purchased from the following commercial sources: Trastuzumab (Herceptin®) was obtained from Genentech, Inc. (South San Francisco, CA), neutral Tris(2-carboxyethyl)phosphine solution from Pierce (Rockford, IL), and NAP™ 5 columns (Sephadex™ G-25 DNA grade) from Amersham Biosciences (Piscataway, NJ). Alexa Fluor® 488 C<sub>5</sub>-maleimide (*Mr.* 721), 680 C<sub>2</sub>-maleimide (*Mr.* ~1000), and 750 C<sub>5</sub>-maleimide (*Mr.* ~1350), and SAIVI™ Alexa Fluor® 680 and 750 Antibody/Protein 1mg-labeling kits were purchased from Invitrogen (Eugene, OR). Centricon® YM-3 and YM-30 and Microcon® YM-3 and YM-30 were obtained from Millipore (Boston, MA). All media and supplements for cell culture were from Invitrogen (Carlsbad, CA).

### Fluorescence conjugation of the HER2-specific Affibody molecules

The Affibody molecules, His<sub>6</sub>- $Z_{\text{HER2:342}}$ -Cys, His<sub>6</sub>-( $Z_{\text{HER2:477}}$ )<sub>2</sub>-Cys, and ABD-( $Z_{\text{HER2:342}}$ )<sub>2</sub>-Cys, contain a unique C-terminal cysteine residue that allows for site-specific labeling (12). This cysteine was used to fluorescently label the Affibody molecules with thiol-reactive Alexa Fluor-maleimide dyes. To reduce oxidized cysteines prior to conjugation, the Affibody molecules were incubated with 5 mmol/L neutral TCEP at pH 7.4 for 20 min at room temperature. Immediately after reduction, Alexa Fluor-maleimide dyes dissolved in DMSO were added and conjugation completed according to the manufacturer's protocol. Unreacted Alexa Fluor-maleimide dyes were removed by passage through a NAP-5 desalting column. Final traces were removed by concentrating and washing with a Centricon YM3 filter unit. All procedures were performed under dimmed light. The molecular weights of the sample proteins were analyzed by SDS-PAGE and the degree of labeling calculated based on the company's instructions.

Trastuzumab was also conjugated with Alexa Fluor dye according to a protocol from the SAIVI™ Alexa Fluor 680 and 750 Antibody/Protein 1mg-labeling kit. Briefly, Alexa Fluor NHS esters were incubated with the protein in a basic medium (pH 9.3). Labelled protein (trastuzumab) was isolated and purified by gel filtration. The final dye-to-protein ratio (number of Alexa Fluor molecules coupled to each protein molecule) was determined to be between 2.5 and 3.5, according to a protocol from Invitrogen. All of the fluorescently labeled protein samples were aliquoted and stored in the dark at -70°C.

### *In vitro* binding affinity measurement of the Affibody conjugates using surface plasmon resonance

Surface plasmon resonance (SPR) experiments were performed on a BIACORE T100 instrument (Biacore Inc., Piscataway, NJ) by long (33 min) injection. For HER2/FC (R&D Systems, Minneapolis, MN; 10 µg/mL in HBS-EP buffer), 1500 RU of protein were captured on the protein A/G modified CM5 sensor chip via an immobilization capture wizard. A concentration series of  $Z_{\text{HER2:342}}$  were injected for 33 min over the HER2/FC capture surface at 5 µL/min (26). To verify the consistency of the kinetic data, we plotted the RU response against the Affibody concentration and fit the data to the four-parameter logistics equation in BIA evaluation software version 3.1. The SPR instruments show a number of instrument effects, as well as binding activity, in the recovered signals. These effects are often removed through a double referencing protocol (27). The data were fitted

using a simple one-to-one interaction model with non-zero initial conditions, and apparent  $K_D$  estimates were recovered.

### Cell cultures

The human breast adenocarcinoma SKBR-3, the human breast ductal carcinoma BT-474, and the human ovarian adenocarcinoma SKOV-3 were obtained from the American Type Culture Collection (ATCC; Manassas, VA). Human glioblastoma U251 MG cells were kindly provided by Dr. Kevin Camphausen (ROB, NCI, Bethesda, MD). The selection of cell lines was based on (a) the possibility and ease of generating xenografts and (b) the HER2 expression levels. BT474, SKBR-3 and SKOV-3 cells were chosen as cell lines with a high HER2 expression level (+4 to +5) and the U251 MG cell line was chosen as a negative control. All cells were maintained in culture media at 37°C at 5% CO<sub>2</sub> in a humidified environment. SKBR-3 and SKOV-3 cells were grown in McCoy's 5A supplemented with 10% fetal bovine serum (FBS) and Pen/Strep (10,000 U penicillin, 10 mg streptomycin). BT-474 and U251 MG were grown in DMEM supplemented as described above. The cells were detached from culture plates with a solution of 0.05% trypsin and 0.02% EDTA in PBS (Invitrogen).

### Cell proliferation assay

The Cell Counting Kit-8 (CCK-8) Assay (Dojindo, Gaithersburg, MD) was used to analyze the effect of Affibody molecules and/or trastuzumab on cell viability *in vitro*. Cells were plated in 96-well flat bottom plates at a density of  $1-2 \times 10^3$  cells/100  $\mu$ L of growth medium. Affibody molecules and trastuzumab were dissolved in PBS at 1 and 20 mg/mL, respectively. These stocks were further serially diluted in tissue culture media and 100  $\mu$ L of each added directly to cell cultures previously plated into 96-well plates. Cells were incubated for two days after treatments at increasing concentrations from 1 nmol/L to 10  $\mu$ mol/L. The results were expressed as the relative percentage of absorbance compared with untreated controls.

### Clonogenic survival assay

Cells were seeded at 200–500 per well of 6-well plates and left to attach for two days. Affibody or trastuzumab was diluted with the growth media to concentrations of 0.1 and 1  $\mu$ mol/L, respectively, and 2 mL of each were added to each well. Control cells were not treated with either drug. Three days after treatments, the media were replaced by a drug-free medium. Following the addition of the drug-free medium, the cells were left to grow until colonies were visible. The cells were cultured for 14 days, with a media change every three days. Colonies containing more than 50 cells were counted. Plating efficiency was calculated as number of colonies per well divided by number of cells plated and survival fraction was obtained by normalization to the untreated controls.

### Confocal Microscopy and Flow cytometry analysis

Cultured cells were incubated with fluorescently labeled conjugates at 37°C for the indicated times. The detection of labeled cells was verified using established *in vitro* fluorescence methods. Flow cytometry was done using a FACSCalibur instrument (BD Biosciences, San Jose, CA) equipped with an argon-ion laser and an optional second red diode laser; source energy, 15 mW; detection time, 500 counts per second). Cell Quest software was used for data acquisition and analysis. Ten thousand cells were gated. Data were live-gated by FL1 (blue laser, 488 nm) and FL4 (red laser 635 nm).

The different groups were also investigated qualitatively by laser scanning microscopy. The cells were analyzed using the 633-nm He–Ne Laser (source energy, 15 mW; LASOS, Jena,

Germany) at 100% for excitation and the LP650 filter of the LSM510 (Zeiss, Jena, Germany). All images were recorded using identical settings.

## Animals

Female athymic nude mice (nu/nu genotype, BALB/c background) approximately five to eight weeks old were used. This study was approved by Animal Safety and Use Committee of National Institutes of Health (Animal Study Proposal ROB#117). Mice were cared for and treated in accordance with the United States Department of Health and Human Services Guide for the Care and Use of Laboratory Animals.

## Subcutaneous tumor xenografts

Tumor cells were implanted into the right flanks of athymic mice. Briefly,  $5\text{--}10 \times 10^6$  cells in 0.2 mL of 50% Matrigel (BD Biosciences, Bedford, MA) were injected subcutaneously into the right flanks. Tumor size was measured periodically using calipers and the tumors allowed to grow to approximately 7 mm in diameter. The typical weight of the xenografts used for the imaging study was 100–300 mg.

## In vivo near-infrared optical imaging

Fluorescence intensity was quantified using a NIR fluorescence small-animal imager, the details of which have been described elsewhere (28). Briefly, the system was based on a time-domain technique, where an advance time-correlated single-photon counting device was used in conjunction with a high-speed repetition-rate tunable laser to detect individual photons. The imager had a laser source for fluorescence excitation ( $\lambda = 750$  nm), an emission filter ( $\lambda = 780$  nm) for fluorescence detection, and a computer for data analysis. A cooled, charge-coupled device (CCD) camera was also used to guide the scan to the region of interest (ROI) and to measure the fluorescence intensity distribution, which helped to locate the tumor inside the tissue.

To analyze the specific target accumulation of the imaging probes, mice were anesthetized by inhalation of isoflurane. Ten micrograms of Affibody conjugates or 50  $\mu\text{g}$  of Trastuzumab conjugates were injected into the tail vein and imaged at predetermined time points after injection ( $n = 3$  in each group). For the blocking experiment, 1 mg of unlabeled Affibody or 5 mg of unlabeled trastuzumab were injected into the tail vein 1 h before the injection of labeled conjugates. The fluorescence signal mean and standard deviation were calculated by averaging the maximum pixel values over the tumor area and corresponding contralateral site. Unless otherwise indicated, three independent experiments were performed.

## RESULTS

### Cellular toxicity of trastuzumab and HER2-specific Affibody molecules

In order to evaluate the toxicity of HER2-specific Affibody proteins, their effects on cell proliferation and clonogenic survival were assessed. Two cancer cell lines known to overexpress the HER2 receptor, SKBR-3 and SKOV-3, were used for this study. Incubation of these cells with the Affibody for 48 h did not significantly inhibit cell growth and proliferation in any concentration range tested (1 nmol/L to 10  $\mu\text{mol/L}$ ); however, trastuzumab did inhibit cell growth and proliferation in a dose-dependent manner, up to 20% during a 48 h incubation period in both cell lines. Simultaneous exposure to Affibody molecules and trastuzumab did not change the effect of the latter on the cells' proliferation (Fig. 1A). Clonogenic survival assays showed similar results, suggesting that the Affibody did not significantly affect the clonogenic survival of these cells 2 weeks after the treatment, whereas trastuzumab did decrease clonogenic survival to 50% (Fig. 1B). Affibody as well as

trastuzumab did not induce any significant effect on HER2-negative U251 cells as expected (Data not shown).

### Fluorescence conjugation of HER2-specific Affibody molecules

Thiol-reactive conjugation with maleimide-containing dyes was adopted for our study because a unique C-terminal cysteine residue had been incorporated into the Affibody protein by the manufacturer to allow site-specific labeling (Supplementary Fig S1A). This cysteine residue was used to fluorescently label the Affibody proteins with thiol-reactive Alexa Fluor-maleimide dyes. Prior to conjugation, the Affibody proteins had to be reduced to expose their free sulfhydryl groups because some of the proteins had formed dimers during storage (Supplementary Fig S1B). Estimated labeling efficiencies of the final, labeled Affibody conjugates ranged from 60 to 80%, based on assessments by silver staining and spectroscopic absorbance measurements, assuming a 1:1 labeling reaction. Trastuzumab was also conjugated with Alexa Fluor 680 and 750 using commercially available kits. The degree of labeling for the trastuzumab conjugates was estimated at 2.5 to 3.5, based on the manufacturer's instruction.

### Measurement of *in vitro* binding affinities of the Affibody conjugates

Biacore analysis was performed without regeneration of the HER2 capture surface due to surface instability. Since the reported  $K_D$  of  $Z_{HER2:342}$  was 22 pmol/L (24), the Affibody was tested at a concentration range of 7.8 pmol/L to 0.5 nmol/L, in 2-fold dilutions, to encompass the equilibrium constant. Representative data are shown in Supplementary Fig S1C. The titration series of the Alexa Fluor labeled Affibody worked well enough to see saturation binding of the surface, but the binding affinity was somewhat less than the unlabeled Affibody  $Z_{HER2:342}$ . The calculated  $K_D$  values and rate constants are presented in Table 1.

### FACS analysis

In order to assess the binding specificities and patterns of the fluorescence-labeled Affibody conjugates, flow cytometry was performed with two different types of human cancer cell lines. The breast adenocarcinoma cell line SKBR-3 overexpresses the HER2 receptor and the brain glioblastoma cell line U251 MG does not express the HER2 receptor. After labeling SKBR-3 cells with Affibody-Alexa Fluor 488 conjugate, cell sorting revealed HER2 receptor-specific and high affinity binding of the conjugate. As shown in Fig. 2A and Supplementary Table S1, 5 nmol/L of the conjugate was bound to 94.6% of cells and 50 nmol/L of the conjugate bound to 98.9% of cells. These results, together with the results of separate experiments using 1, 10, and 100 nmol/L of the conjugate (data not shown), indicated high affinity binding with saturation at concentrations lower than 10 nmol/L. Alexa Fluor dyes themselves did not bind to any of the cells (1.1% for SKBR-3 cells and 0.9% for U251 MG cells). A blocking experiment that included preincubation with a 100-fold excess of unlabeled Affibody showed almost complete binding inhibition (0.8% with 5 nmol/L and 1.1% with 50 nmol/L), suggesting that the conjugate competes with unlabeled Affibody and is specific to the HER2 receptor. Non-HER2-expressing U251 MG cells failed to show any significant binding to the Affibody conjugate under all conditions tested, confirming the specificity of the HER2 receptor.

As shown in Fig. 2B and Supplementary Table S2, double-labeling of cells with the Affibody-Alexa Fluor 488 and trastuzumab-Alexa Fluor 680 conjugates further demonstrated that their binding is HER2 receptor-specific and independent of each other, indicating that the binding epitopes are separate and different. Blocking the binding with excess unlabeled Affibody or trastuzumab showed almost complete binding inhibition of the corresponding conjugate (97.0% when blocked with Affibody and 98.3% when blocked with

trastuzumab), while the binding of the other conjugate was not blocked. The binding of both conjugates was also completely inhibited in the presence of the two blockers (97.4%). It also showed that the non-HER2-expressing U251 MG cells did not bind the conjugates in any of the treatments.

### Confocal microscopy

Confocal microscopy experiments were performed to further investigate the binding specificities and patterns of the Affibody and trastuzumab conjugates. After double-labeling cells with the Affibody-Alexa Fluor 488 and trastuzumab-Alexa Fluor 680 conjugates, confocal images showed an almost exclusive binding of the conjugates to cell surface membranes. The images were perfectly merged on the same field, demonstrating that their binding occurred in the same region (Fig. 3A). Blocking with 100-fold excess amounts of unlabeled Affibody or trastuzumab resulted in an almost complete absence of fluorescence from the corresponding conjugate, while the fluorescence from other conjugate did not change. The binding of both conjugates was also completely inhibited in the presence of the two blockers (unconjugated Affibody and trastuzumab) suggesting that the conjugates are specific to HER2 receptors and the binding of the two conjugates occurs independently. Because it is known that trastuzumab can be internalized into the cells, the study was further extended to see whether the Affibody conjugate can also enter the cells. To address this question, the labeling incubation time was prolonged, up to 6 hours, and confocal images generated. As shown in Fig. 3B, the images suggested that both conjugates could be internalized by the cells, and that the internalization was time-dependent because more fluorescence was seen inside cells at 6 hours compared to the fluorescence seen at 1 and 3 hours. In contrast, non-HER2-expressing U251 MG cells failed to show any significant fluorescence from the two conjugates in any cellular regions.

### *In vivo* near-infrared optical imaging

Finally, Alexa Fluor 750-conjugated Affibody molecules and trastuzumab were tested as NIR probes for *in vivo* optical imaging using HER2-overexpressing tumor mouse xenografts. We investigated which form of HER2-specific Affibody molecules could be best candidate among three different forms available from the company (monomer, dimer and albumin-binding domain-fused dimer). Examples of mouse whole body images measured by CCD camera at different time points after tail vein injection of the trastuzumab-Alexa Fluor 750, Affibody ABD-(Z<sub>HER2:342</sub>)<sub>2</sub>-Alexa Fluor 750, and Affibody Z<sub>HER2:342</sub> monomer-Alexa Fluor 750 are shown in Fig. 4A. The pharmacokinetics of each probe in the tumor area and contralateral normal tissue area were quantified using a fiber optic device and averaged. Corresponding graphs are shown in Fig. 4B. Mice injected with the trastuzumab-Alexa Fluor 750 conjugate showed moderate fluorescence intensities at first around the tumor and liver area, until the 24 h time point. Localization of the signal intensities in the tumor area became increasingly evident and intense after 24 h and peaked around 48 h. After that, the signals from the tumor area lasted up to 2 weeks, while slowly growing weaker. On the contrary, mice injected with the Affibody ABD-(Z<sub>HER2:342</sub>)<sub>2</sub>-Alexa Fluor 750 showed high, intense signals around the tumor and kidney area until the 8 h time point. Accumulation of the signals in the tumor area became evident and remained intense around 24 h and peaked before 48 h. After peaking, the signals from the tumor area decreased gradually and almost disappeared after 72 h. However, mice injected with the Affibody monomer Z<sub>HER2:342</sub>-Alexa Fluor 750 showed high fluorescence intensities only in the kidney area until 4 h, and tumor signals were washed out quickly, even though weak, localized signals were detected around 6 to 8 h. Most signal intensities were cleared after 24 h. Signal-to-background ratios (SBRs) of each probe from peak post-injection times were calculated by normalizing signals from tumor area to those from contralateral normal tissue area. The SBRs were highest in Affibody ABD-(Z<sub>HER2:342</sub>)<sub>2</sub>-Alexa Fluor 750, followed by

trastuzumab-Alexa Fluor 750, and Affibody monomer  $Z_{\text{HER2}:342}$ -Alexa Fluor 750 (Table 2). The clearance rates of each probe in the tumor area were calculated based on the derived equations after fitting each curve to single exponential decay. The derived half-lives were also shown in Table 2. As expected, the half-life was longest with the trastuzumab-Alexa Fluor 750 conjugate (108 h), followed by Affibody ABD- $(Z_{\text{HER2}:342})_2$ -Alexa Fluor 750 (45 h), and Affibody monomer  $Z_{\text{HER2}:342}$ -Alexa Fluor 750 (11 h).

The fluorescence intensities from each isolated tissue, 24 h after the injection of Affibody ABD- $(Z_{\text{HER2}:342})_2$ -Alexa Fluor 750 conjugate, were also measured using a fiber optic device and compared to see whether our *in vivo* measurements reflect the signal intensities from the tumor and other tissues (Fig. 4C). The tumor signal intensity was the highest, with those from the kidney and liver showing the second and third highest levels. All other tissues showed minimal intensities. To validate the specificity of the Affibody ABD- $(Z_{\text{HER2}:342})_2$ -Alexa Fluor 750, we performed the blocking experiment as we did with the cultured cells. One group of mice was preinjected with an excess amount (100-fold) of unlabeled Affibody ABD- $(Z_{\text{HER2}:342})_2$  and another group of mice was preinjected with the same excess of unlabeled trastuzumab 30 min before injection with the Affibody ABD- $(Z_{\text{HER2}:342})_2$ -Alexa Fluor 750 conjugate. The kinetics of the fluorescence intensities in the tumor and contralateral normal tissue area were then measured over time using a fiber optic device (Fig. 4D). Preinjecting the mice with an excess amount of unlabeled Affibody ABD- $(Z_{\text{HER2}:342})_2$  blocked most of the fluorescent signals from the Affibody ABD- $(Z_{\text{HER2}:342})_2$ -Alexa Fluor 750 conjugate, whereas preinjecting with an excess amount of unlabeled trastuzumab failed to block the signals. Specificity of our HER2 imaging analyses were further strengthened by the experiments with HER2-nonexpressing U251 tumors as shown in Fig. 4E.

## DISCUSSION

Molecular imaging has its roots in nuclear medicine, which focuses on the management of patients through the use of radiotracers in conjunction with imaging technologies, such as positron emission tomography (PET) and single photon emission tomography (SPECT). The underlying principle can now be tailored to other imaging modalities, such as optical imaging. Recent, fast-moving trends in this field will allow us to establish noninvasive, specific, sensitive, quantitative, and cost-effective NIR optical imaging techniques. One goal is to provide an ideal probe for HER2 imaging in living animals and, ultimately, in humans. HER2-specific Affibody molecules have been demonstrated to be good candidates for *in vivo* molecular imaging using radionuclide modalities (13–17). However, there is a lack of information regarding the application of these HER2-specific Affibody molecules to *in vivo* NIR optical imaging. In this study, we assessed the feasibility of using of HER2-specific Affibody molecules to create an NIR probe for *in vivo* optical imaging of HER2.

Since part of the goal is to provide probes that will minimally interfere with the studied system, we have examined what effects HER2-specific Affibody molecules might have on the target cells, and whether or not their binding to HER2 interferes with trastuzumab binding and its therapeutic effects. As a first step toward this goal, we assessed the cellular toxicity of HER2-specific Affibody molecules, since, to be an ideal candidate, the probe should minimally affect the target cells. Our data show that the HER2-specific Affibody is not toxic to HER2-expressing cells, while treatment with trastuzumab significantly decreased the viability of the same cells. Furthermore, the presence of the Affibody molecules did not affect the trastuzumab toxicity (Fig. 1). Our results agree with previous findings on cellular toxicity and intracellular signaling pathways (29, 30), supporting our claim that our probe does not affect the system to be studied.



It has been well documented that conjugation chemistry using a maleimide group to react with a thiol group is an efficient method of conjugation (23, 31). It can create a specific 1:1 labeling of proteins with fluorescent dyes if the protein contains only one cysteine residue, like the HER2-specific Affibody used in this study. As shown in Table 1, modification of the HER2-specific Affibody molecules with Alexa Fluor-maleimide dyes resulted in a slight reduction of the apparent affinity of the conjugates, perhaps due to steric hindrance. However, the reduction was minor and the conjugate still showed a picomolar range of affinity to HER2, so it still has a better affinity than trastuzumab (which exhibits a nanomolar range of affinity to HER2). Through competition studies, we have demonstrated that the epitope recognized by the HER2-specific Affibody is distinct from the epitope recognized by trastuzumab. This would allow the use of the HER2-specific Affibody-based reagents to test for changes in HER2 receptor expression in response to trastuzumab therapy. Our data from FACS and confocal microscopy studies showed clearly that trastuzumab and Affibody molecules do not compete for binding to HER2 (Figs. 2 and 3). Taken together, these data demonstrate that the two conjugates are highly HER2 receptor specific and that their HER2 binding epitopes are separate and distinct.

The advantage of an optical method is that it does not involve radioactive materials and is relatively easy to use. Moreover, due to its low absorption in tissue, the NIR optical methods allow us to target even deeply located targets. During the last decade, advanced mathematical modeling (32–35) of propagation of light in tissue and technological improvements of sources and detectors has made possible optical imaging for clinical application. There are several optical methods and systems in use today in clinic where light can penetrate more than 10 cm deep inside the breast tissue using transillumination measurement (36, 37). Additionally, techniques have made possible the application of tomographic principles for imaging of diffuse light (38–41).

In this study, optical imaging system presented for preclinical studies on small animal to study new drug. The current time-domain optical system (28) can be extended for clinical use similar to the Rinneberg group (37) and softScan (Advanced Research Technologies Inc. Montreal, Canada) (42). The unique advantage of our system is that its fixed source-detector separations allow us to obtain signals at different depths in the medium. In conjunction with the time-resolved system, a cooled CCD camera allows the acquisition of a fluorescence image superimposed on a gray-scale photographic image of the small animal using an overlay.

Pharmacokinetics of trastuzumab conjugate was consistent with previous findings by other groups using different fluorophores, thus verifying our imaging system (43, 44). On the contrary, Affibody monomer  $Z_{\text{HER2:342}}$ -Alexa Fluor 750 conjugate failed to show clear signs of tumor accumulation and fast clearance. Instead it showed fast accumulation in the kidney. Previous reports on the use of Affibody monomer  $Z_{\text{HER2:342}}$  in radionuclide imaging also showed fast clearance from the blood and instant uptake into the kidney, but they reported tumor accumulation within several hours after injection (24, 25). Our conflicting data for this aspect could be due to differences in chemical nature between our fluorescent dye and their radiotracers, or differences in the imaging modalities. In our hands, there was no improvement in tumor accumulation of the Affibody monomer  $Z_{\text{HER2:342}}$ -Alexa Fluor 750 conjugate, even with different batches and different dosages (data not shown). Furthermore, the dimer form of the Affibody conjugate also failed to show clear tumor accumulation (data not shown). Fusion of the albumin-binding domain (ABD) to imaging probes has been successfully adopted to prolong the circulation half-life of the probes, including the HER2-specific Affibody molecule (45, 46). With the use of Affibody ABD- $(Z_{\text{HER2:342}})_2$ -Alexa Fluor 750 conjugate, we finally observed clear signs of tumor accumulation with an extended half-life. These results showed that the Affibody ABD-

(Z<sub>HER2:342</sub>)<sub>2</sub> conjugate was the best performer for *in vivo* NIR optical imaging, in terms of tumor accumulation and clearance, compared to the trastuzumab and Affibody monomer and dimer conjugates.

To our knowledge, this is the first report on the quantitative *in vivo* NIR optical imaging of HER2-expressing tumors using Affibody molecules. This approach should provide the opportunity for the development of a rapid and cost-effective imaging modality as an improvement over costly radionuclide-based imaging modalities. A noninvasive paradigm for molecular imaging could provide a new tool for optimization of HER2-targeted therapies using preclinical animal models and a unique non-invasive means for *in vivo* characterization of HER2 expression in patients and possible monitoring of their downregulation in response to therapeutic interventions. The application of our probe to a combination of conventional and HER2-specific molecular therapies may provide new approaches in the treatment of HER2-positive breast cancer.

## Supplementary Material

Refer to Web version on PubMed Central for supplementary material.

## Acknowledgments

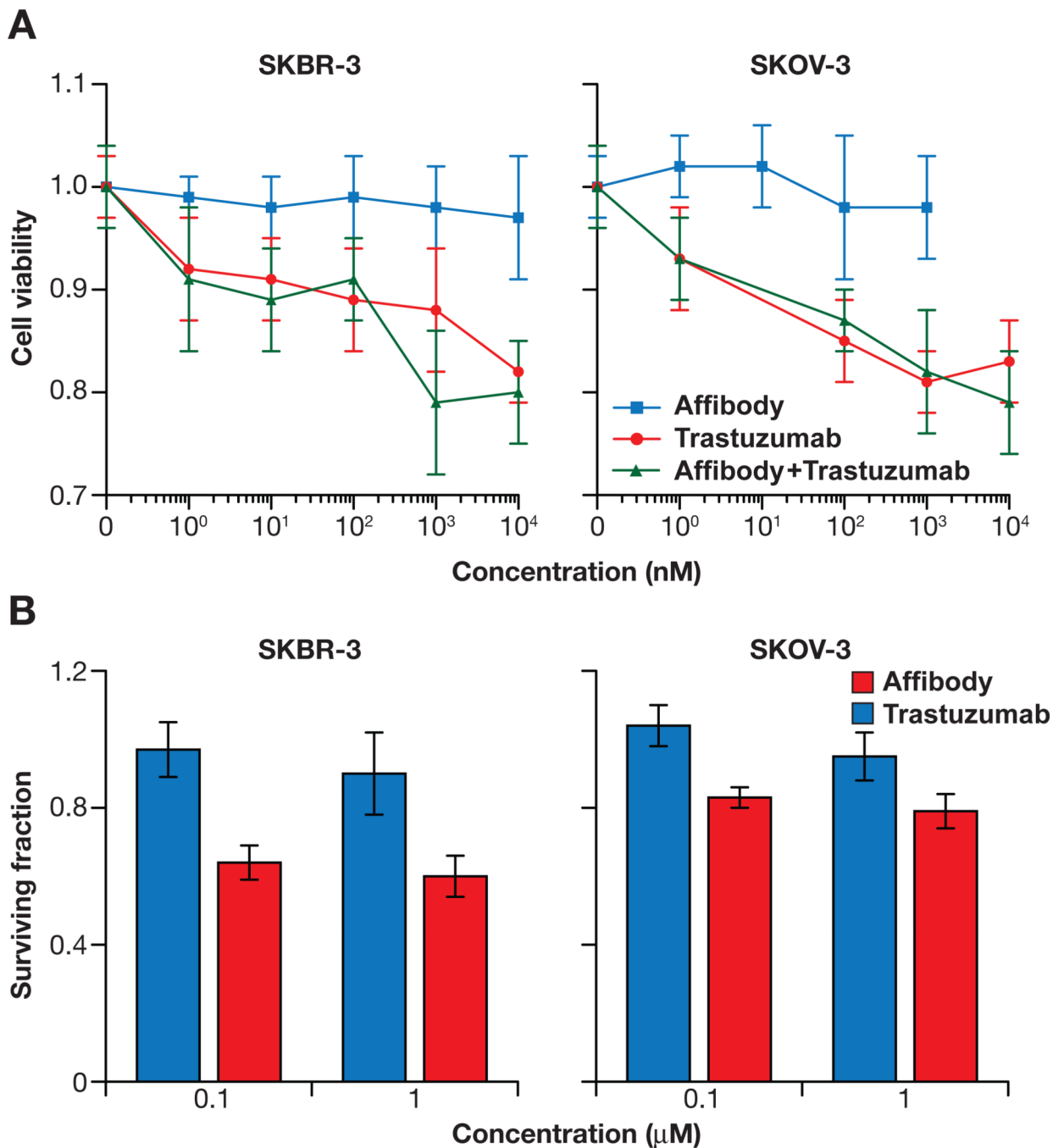
The authors appreciate the support of Affibody AB. We also thank Michael Kruhlik for confocal microscopy, Barbara Joan Taylor for FACS, and Lesa Holly for general laboratory assistance. This research was supported in part by the Center for Cancer Research, an Intramural Research Program of the National Cancer Institute, National Institute of Child Health and Human Development, and by Breast Cancer Research Stamp Fund awarded through competitive peer review, and was funded in part with Federal funds from the National Cancer Institute, National Institutes of Health, under Contracts N01-CO-12400 and N01-CO-12401. The content of this publication does not necessarily reflect the views or policies of the Department of Health and Human Services, nor does mention of trade names, commercial products, or organization imply endorsement by the U.S. Government.

## REFERENCES

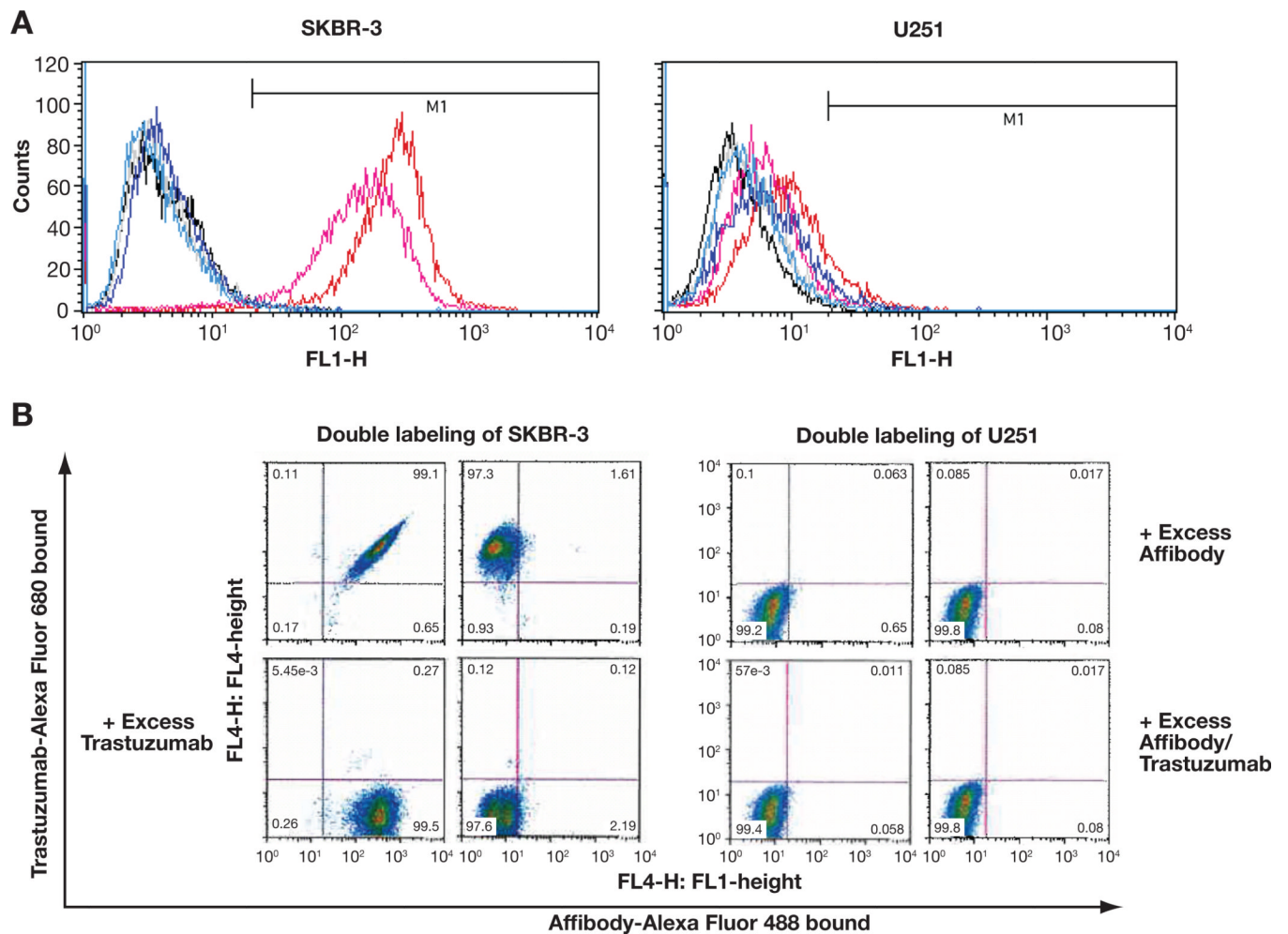
1. Slamon DJ, Clark GM, Wong SG, Levin WJ, Ullrich A, McGuire WL. Human breast cancer: correlation of relapse and survival with amplification of the HER-2/neu oncogene. *Science*. 1987; 235:177–182. [PubMed: 3798106]
2. Witton CJ, Reeves JR, Going JJ, Cooke TG, Bartlett JM. Expression of the HER1-4 family of receptor tyrosine kinases in breast cancer. *J Pathol*. 2003; 200:290–297. [PubMed: 12845624]
3. Hynes NE, Lane HA. ERBB receptors and cancer: the complexity of targeted inhibitors. *Nat Rev Cancer*. 2005; 5:341–354. [PubMed: 15864276]
4. Adams GP, Weiner LM. Monoclonal antibody therapy of cancer. *Nat Biotechnol*. 2005; 23:1147–1157. [PubMed: 16151408]
5. Dancey JE, Chen HX. Strategies for optimizing combinations of molecularly targeted anticancer agents. *Nat Rev Drug Discov*. 2006; 5:649–659. [PubMed: 16883303]
6. Nahta R, Yu D, Hung MC, Hortobagyi GN, Esteva FJ. Mechanisms of disease: understanding resistance to HER2-targeted therapy in human breast cancer. *Nat Clin Pract Oncol*. 2006; 3:269–280. [PubMed: 16683005]
7. Laudadio J, Quigley DI, Tubbs R, Wolff DJ. HER2 testing: a review of detection methodologies and their clinical performance. *Expert Rev Mol Diagn*. 2007; 7:53–64. [PubMed: 17187484]
8. Zidan J, Dashkovsky I, Stayerman C, Basher W, Cozacov C, Hadary A. Comparison of HER-2 overexpression in primary breast cancer and metastatic sites and its effect on biological targeting therapy of metastatic disease. *Br J Cancer*. 2005; 93:552–556. [PubMed: 16106267]
9. Herschman HR. Molecular imaging: looking at problems, seeing solutions. *Science*. 2003; 302:605–608. [PubMed: 14576425]

10. Olafsen T, Kenanova VE, Sundaresan G, et al. Optimizing radiolabeled engineered anti-p185HER2 antibody fragments for in vivo imaging. *Cancer Res.* 2005; 65:5907–5916. [PubMed: 15994969]
11. Robinson MK, Doss M, Shaller C, et al. Quantitative immuno-positron emission tomography imaging of HER2-positive tumor xenografts with an iodine-124 labeled anti-HER2 diabody. *Cancer Res.* 2005; 65:1471–1478. [PubMed: 15735035]
12. Lundberg E, Hoiden-Guthenberg I, Larsson B, Uhlen M, Graslund T. Site-specifically conjugated anti-HER2 Affibody molecules as one-step reagents for target expression analyses on cells and xenograft samples. *J Immunol Methods.* 2007; 319:53–63. [PubMed: 17196217]
13. Tolmachev V, Orlova A, Nilsson FY, Feldwisch J, Wennborg A, Abrahmsen L. Affibody molecules: potential for in vivo imaging of molecular targets for cancer therapy. *Expert Opin Biol Ther.* 2007; 7:555–568. [PubMed: 17373906]
14. Wikman M, Steffen AC, Gunneriusson E, et al. Selection and characterization of HER2/neu-binding affibody ligands. *Protein Eng Des Sel.* 2004; 17:455–462. [PubMed: 15208403]
15. Perik PJ, Lub-De Hooge MN, Gietema JA, et al. Indium-111-labeled trastuzumab scintigraphy in patients with human epidermal growth factor receptor 2-positive metastatic breast cancer. *J Clin Oncol.* 2006; 24:2276–2282. [PubMed: 16710024]
16. Smith-Jones PM, Solit DB, Akhurst T, Afroze F, Rosen N, Larson SM. Imaging the pharmacodynamics of HER2 degradation in response to Hsp90 inhibitors. *Nat Biotechnol.* 2004; 22:701–706. [PubMed: 15133471]
17. Nilsson FY, Tolmachev V. Affibody molecules: new protein domains for molecular imaging and targeted tumor therapy. *Curr Opin Drug Discov Devel.* 2007; 10:167–175.
18. Hoffman RM. The multiple uses of fluorescent proteins to visualize cancer in vivo. *Nat Rev Cancer.* 2005; 5:796–806. [PubMed: 16195751]
19. Shaner NC, Steinbach PA, Tsien RY. A guide to choosing fluorescent proteins. *Nat Methods.* 2005; 2:905–909. [PubMed: 16299475]
20. Frangioni JV. In vivo near-infrared fluorescence imaging. *Curr Opin Chem Biol.* 2003; 7:626–634. [PubMed: 14580568]
21. Graves EE, Weissleder R, Ntziachristos V. Fluorescence molecular imaging of small animal tumor models. *Curr Mol Med.* 2004; 4:419–430. [PubMed: 15354872]
22. Montet X, Ntziachristos V, Grimm J, Weissleder R. Tomographic fluorescence mapping of tumor targets. *Cancer Res.* 2005; 65:6330–6336. [PubMed: 16024635]
23. Tada H, Higuchi H, Wanatabe TM, Ohuchi N. In vivo real-time tracking of single quantum dots conjugated with monoclonal anti-HER2 antibody in tumors of mice. *Cancer Res.* 2007; 67:1138–1144. [PubMed: 17283148]
24. Orlova A, Magnusson M, Eriksson TL, et al. Tumor imaging using a picomolar affinity HER2 binding affibody molecule. *Cancer Res.* 2006; 66:4339–4348. [PubMed: 16618759]
25. Orlova A, Tolmachev V, Pehrson R, et al. Synthetic affibody molecules: a novel class of affinity ligands for molecular imaging of HER2-expressing malignant tumors. *Cancer Res.* 2007; 67:2178–2186. [PubMed: 17332348]
26. Karlsson R, Katsamba PS, Nordin H, Pol E, Myszkka DG. Analyzing a kinetic titration series using affinity biosensors. *Anal Biochem.* 2006; 349:136–147. [PubMed: 16337141]
27. Myszkka DG. Improving biosensor analysis. *J Mol Recognit.* 1999; 12:279–284. [PubMed: 10556875]
28. Hassan M, Riley J, Chernomordik V, et al. Fluorescence lifetime imaging system for in vivo studies. *Mol Imaging.* 2007; 6:229–236. [PubMed: 17711778]
29. Ekerljung L, Steffen AC, Carlsson J, Lennartsson J. Effects of HER2-binding affibody molecules on intracellular signaling pathways. *Tumour Biol.* 2006; 27:201–210. [PubMed: 16651854]
30. Konecny GE, Pegram MD, Venkatesan N, et al. Activity of the dual kinase inhibitor lapatinib (GW572016) against HER-2-overexpressing and trastuzumab-treated breast cancer cells. *Cancer Res.* 2006; 66:1630–1639. [PubMed: 16452222]
31. Mume E, Orlova A, Larsson B, et al. Evaluation of ((4-hydroxyphenyl)ethyl)maleimide for site-specific radiobromination of anti-HER2 affibody. *Bioconjug Chem.* 2005; 16:1547–1555. [PubMed: 16287254]

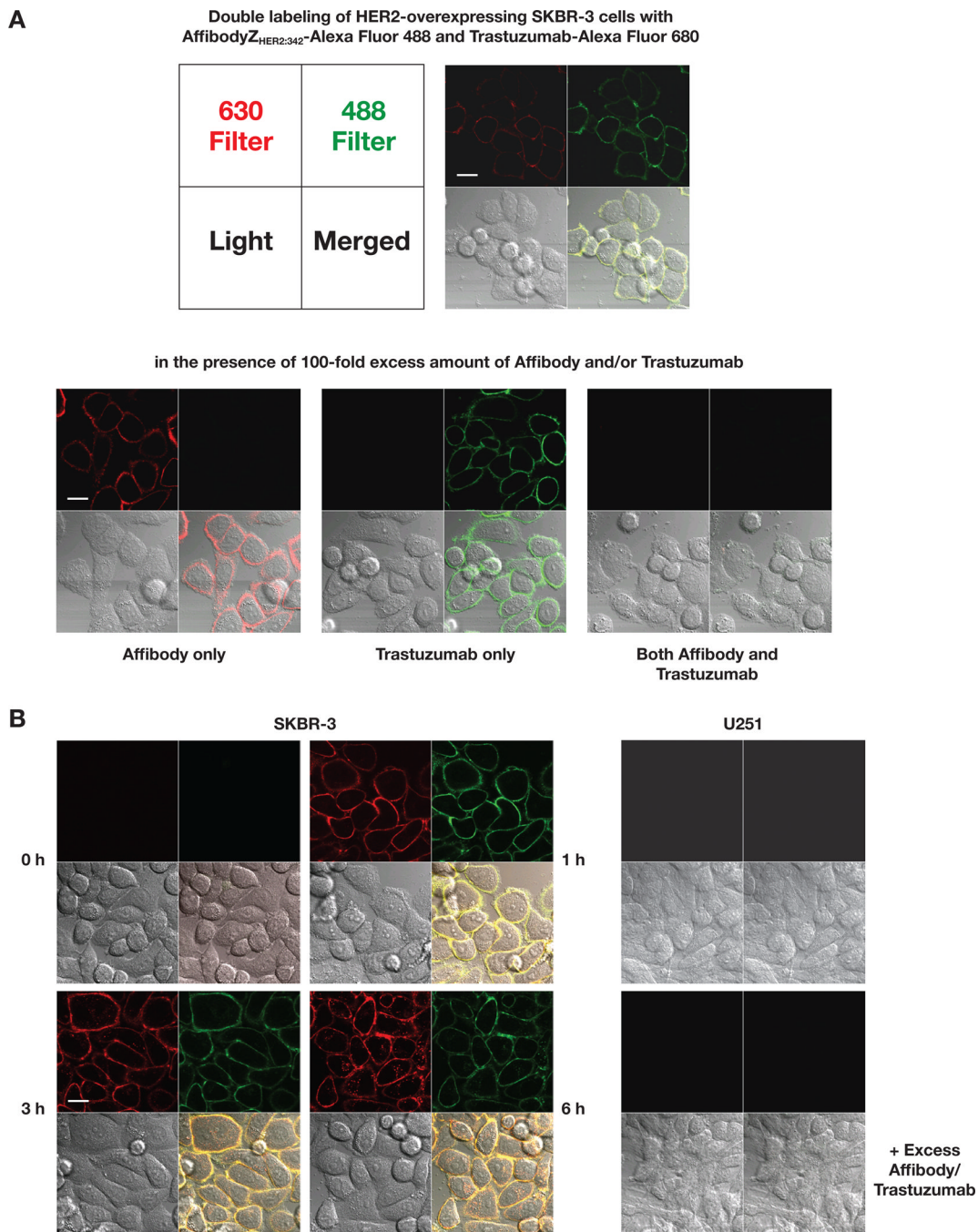
32. Chernomordik V, Gandjbakhche A, Lepore M, Esposito R, Delfino I. Depth dependence of the analytical expression for the width of the point spread function (spatial resolution) in time-resolved transillumination. *J Biomed Opt.* 2001; 6:441–445. [PubMed: 11728203]
33. Chernomordik V, Hattery DW, Gannot I, Zaccanti G, Gandjbakhche A. Analytical calculation of the mean time spent by photons inside an absorptive inclusion embedded in a highly scattering medium. *J Biomed Opt.* 2002; 7:486–492. [PubMed: 12175301]
34. Dudko OK, Weiss GH, Chernomordik V, Gandjbakhche AH. Photon migration in turbid media with anisotropic optical properties. *Phys Med Biol.* 2004; 49:3979–3989. [PubMed: 15470918]
35. Gandjbakhche AH, Chernomordik V, Hattery D, Hassan M, Gannot I. Tissue characterization by quantitative optical imaging methods. *Technol Cancer Res Treat.* 2003; 2:537–551. [PubMed: 14640765]
36. Grosenick D, Moesta KT, Moller M, et al. Time-domain scanning optical mammography: I. Recording and assessment of mammograms of 154 patients. *Phys Med Biol.* 2005; 50:2429–2449. [PubMed: 15901947]
37. Rinneberg H, Grosenick D, Moesta KT, et al. Scanning time-domain optical mammography: detection and characterization of breast tumors in vivo. *Technol Cancer Res Treat.* 2005; 4:483–496. [PubMed: 16173820]
38. Choe R, Corlu A, Lee K, et al. Diffuse optical tomography of breast cancer during neoadjuvant chemotherapy: a case study with comparison to MRI. *Med Phys.* 2005; 32:1128–1139. [PubMed: 15895597]
39. Enfield LC, Gibson AP, Everdell NL, et al. Three-dimensional time-resolved optical mammography of the uncompressed breast. *Appl Opt.* 2007; 46:3628–3638. [PubMed: 17514325]
40. Intes X, Ripoll J, Chen Y, Nioka S, Yodh AG, Chance B. In vivo continuous-wave optical breast imaging enhanced with Indocyanine Green. *Med Phys.* 2003; 30:1039–1047. [PubMed: 12852527]
41. Ntziachristos V, Yodh AG, Schnall M, Chance B. Concurrent MRI and diffuse optical tomography of breast after indocyanine green enhancement. *Proc Natl Acad Sci U S A.* 2000; 97:2767–2772. [PubMed: 10706610]
42. Intes X. Time-domain optical mammography SoftScan: initial results. *Acad Radiol.* 2005; 12:934–947. [PubMed: 16023382]
43. Barrett T, Koyama Y, Hama Y, et al. In vivo Diagnosis of Epidermal Growth Factor Receptor Expression using Molecular Imaging with a Cocktail of Optically Labeled Monoclonal Antibodies. *Clin Cancer Res.* 2007; 13:6639–6648. [PubMed: 17982120]
44. Koyama Y, Hama Y, Urano Y, Nguyen DM, Choyke PL, Kobayashi H. Spectral fluorescence molecular imaging of lung metastases targeting HER2/neu. *Clin Cancer Res.* 2007; 13:2936–2945. [PubMed: 17504994]
45. Dennis MS, Jin H, Dugger D, et al. Imaging tumors with an albumin-binding Fab, a novel tumor-targeting agent. *Cancer Res.* 2007; 67:254–261. [PubMed: 17210705]
46. Tolmachev V, Orlova A, Pehrson R, et al. Radionuclide therapy of HER2-positive microxenografts using a <sup>177</sup>Lu-labeled HER2-specific Affibody molecule. *Cancer Res.* 2007; 67:2773–2782. [PubMed: 17363599]



**Figure 1.** Affibody treatment did not inhibit cell proliferation and growth, in contrast to trastuzumab treatment. *A.* Effect of Affibody on cell viability. Results were expressed as the relative ratio of cell viability compared to untreated control cells. Experimental conditions were tested in quintuplicate (5 wells of the 96-well plate per experimental condition), and independent experiments were performed in triplicate. Data are presented as means  $\pm$  SD. *B.* Effect of Affibody on clonogenic survival. Survival was expressed as a fraction of the controls. Bar graphs shown here present the mean  $\pm$  SD from three independent experiments with triplicates of each group.



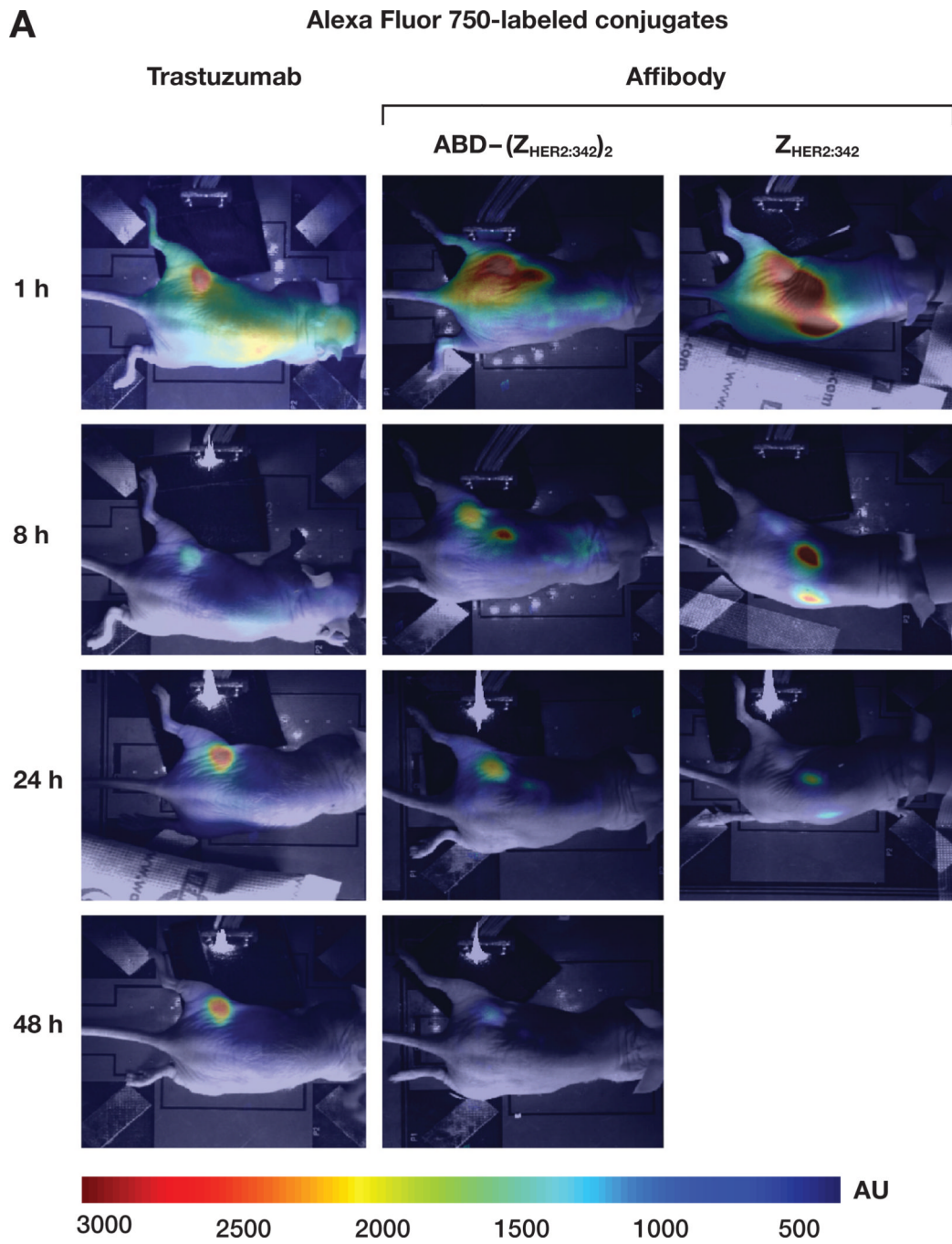
**Figure 2.** Alexa Fluor-labeled Affibody conjugates retained specificity and binding characteristics to HER2. *A.* Flow cytometry after labeling the cells with Affibody  $Z_{\text{HER2}:342}$ -Alexa Fluor 488 showed specific and high-affinity binding of the conjugate to HER2 receptors. Typical representatives of each experiment were shown by overlaid histograms. *B.* FACS analysis after double-labeling of cells with 1 nM of Affibody  $Z_{\text{HER2}:342}$ -Alexa Fluor 488 and 10 nM of Trastuzumab-Alexa Fluor-680 demonstrated specific and independent binding of the conjugate to HER2 receptors. Representatives of each experiment were shown by dot plots.

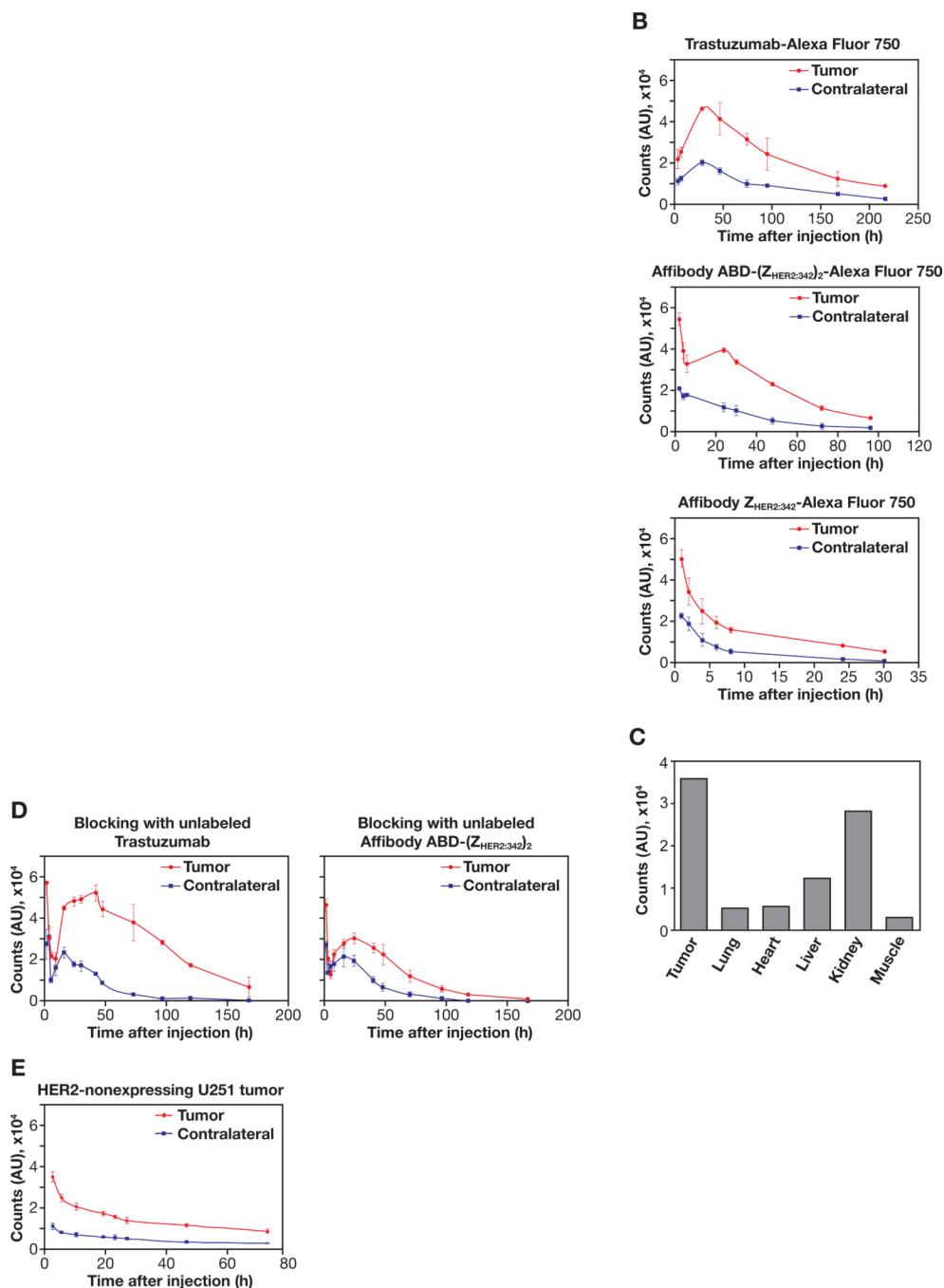


**Figure 3.** Confocal microscopy studies showed specific, independent binding to HER2, and internalization of the Alexa Fluor-labeled Affibody conjugates. *A.* Double-labeling of SKBR-3 cells with 1 nM of Affibody <sub>Z<sub>HER2:342</sub></sub>-Alexa Fluor 488 and 10 nM of Trastuzumab-Alexa Fluor 680. *B. (Left Panel)* Double-labeling of SKBR-3 cells for the indicated time. *(Right Panel)* Double-labeling of U251 cells under the same condition for 1 hr. For the blocking experiments shown at the bottom in each panel, 100-fold excess of unlabeled Affibody and Trastuzumab were added 30 min before the addition the conjugates. Live cell images were recorded using identical settings. All the experiments were done in

duplicate and repeated three times. Images shown here were representatives of each experiment. Bars: 20  $\mu\text{m}$ .





**Figure 4.**

*In vivo* NIR optical imaging of HER2-expressing tumor xenograft mice after tail-vein injection of the Alexa Fluor 750-labeled conjugates. *A*. Typical pseudo-color fluorescence images using CCD camera at different time points obtained from mice after injecting trastuzumab-Alexa Fluor 750, Affibody ABD-(Z<sub>HER2:342</sub>)<sub>2</sub>-Alexa Fluor 750, or Affibody Z<sub>HER2:342</sub>-Alexa Fluor 750 conjugates. Images of trastuzumab-Alexa Fluor 750 conjugate were taken 3 and 6 h after injection instead of 1 and 8 h. *B*. Pharmacokinetics of the Alexa Fluor 750-labeled conjugate over time after injection into HER2-overexpressing SKBR-3 tumor mice. Signal intensities from each probe were measured using a fiber optic device in the tumor and the contralateral sites at given time points and averaged from three mice. The

graphs were plotted as the mean with error bars. *C. Ex vivo* analysis of fluorescence intensities from isolated various tissues 24 h after injection of Affibody ABD-(Z<sub>HER2:342</sub>)<sub>2</sub>-Alexa Fluor 750 conjugate using a fiber optic device. Each bar represents the mean values from three mice and the SDs are less than 5% in all cases. *D.* Blocking experiment of Affibody ABD-(Z<sub>HER2:342</sub>)<sub>2</sub>-Alexa Fluor 750 conjugate. Mice were preinjected with excess amounts of unlabeled Affibody ABD-(Z<sub>HER2:342</sub>)<sub>2</sub> or trastuzumab into the tail vein 30 min before injection of the Affibody ABD-(Z<sub>HER2:342</sub>)<sub>2</sub>-Alexa Fluor 750 conjugate. *E.* Pharmacokinetics of the Alexa Fluor 750-labeled conjugate over time after injection into HER2-nonexpressing U251 tumor mice. Signal intensities were measured using a fiber optic device in tumor and contralateral site at given time points and averaged from three mice. The pharmacokinetic graphs were plotted as mean with error bars.

**Table 1**

Binding affinities of Affibody molecules calculated by Biacore measurement

Affibody type	$K_D$ (pM)	$k_{on}$ ( $M^{-1}s^{-1}$ )	$k_{off}$ ( $s^{-1}$ )
Unlabeled Z <sub>HER2:342</sub>	30 ± 1	$3.3 \times 10^6 \pm 3.6 \times 10^3$	$1.0 \times 10^{-4} \pm 1.4 \times 10^{-7}$
Z <sub>HER2:342</sub> -Alexa Fluor 750 conjugate	190 ± 1	$4.3 \times 10^6 \pm 4.0 \times 10^2$	$8.9 \times 10^{-5} \pm 1.3 \times 10^{-7}$

NOTE: The values are denoted as mean ± SD (n = 3).

Clearance rates in the tumor and signal-to-background ratios in the tumor during peak times of the Alexa Fluor 750-labeled conjugates

**Table 2**

Conjugates	Half-life of clearance (h)	s/n at 2 h	s/n at 4 h	s/n at 24 h	s/n at 48 h
Trastuzumab-Alexa Fluor 750	115.0 ± 18.4			2.3 ± 0.1	2.5 ± 0.2
Affibody ABD-(Z <sub>HER2:342</sub> ) <sub>2</sub> -Alexa Fluor 750	40.5 ± 1.7			3.4 ± 0.7	4.5 ± 1.5
Affibody Z <sub>HER2:342</sub> -Alexa Fluor 750	5.7 ± 1.6	2.2 ± 0.1	2.5 ± 0.9		

NOTE: The clearance rates of each probe in the tumor were calculated by single exponential fit to the data with time (Fig. 4B). Data were obtained from the tumor after subtracting the corresponding contralateral normal tissue as background signal due to blood circulation. The signal-to-background ratios (s/n) for each probe in the tumor during peak times after injection were calculated by dividing signals from tumor area with those from corresponding contralateral normal tissue area (Fig 4B). The values are denoted as mean ± SD (n = 3).